ORIGINAL RESEARCH PAPER

Highly Sensitive Detection of H_2S Molecules Using a TiO_2-Supported Au Overlayer Based Nanosensors: A Van Der Waals Corrected DFT Study

Amirali Abbasi [1, 2, 3] *, Jaber Jahanbin Sardroodi [1, 2, 3]

[1] *Molecular Simulation Laboratory (MSL), Azarbaijan Shahid Madani University, Tabriz, Iran*

[2] *Computational Nanomaterials Research Group (CNRG), Azarbaijan Shahid Madani University, Tabriz, Iran*

[3] *Department of Chemistry, Faculty of Basic Sciences, Azarbaijan Shahid Madani University, Tabriz, Iran*

ABSTRACT

The adsorption of the H_2S molecule on the undoped and N-doped TiO_2 anatase supported Au nanoparticles were studied using density functional theory calculations. The adsorption of H_2S on both Au and TiO_2 sides of the nanoparticle was examined. On the TiO_2 side, the fivefold coordinated titanium site was found to be the most favorable binding site, giving rise to the strong interaction of H_2S with TiO_2 supported Au overlayer. It was found that the central sulfur atom of the H_2S molecule preferentially binds to the fivefold coordinated titanium sites via formation of strong chemical bonds. By substituting nitrogen atom into the oxygen vacancy of TiO_2, significant changes in the bond lengths, bond angles and adsorption energies of the complex systems occur. The adsorption of H_2S on the N-doped TiO_2-supported Au nanoparticle is more favorable in energy than the adsorption on the pristine one, indicating the strong interaction of H_2S with N-doped TiO_2-supported Au. Thus, the N-doped nanoparticle can be utilized as potentially efficient H_2S gas detection device. The substantial overlaps between the projected density of states of the titanium and sulfur atoms indicate, the formation of a chemical bond between the nanoparticle and H_2S molecule. This work not only proposes a theoretical basis for gas sensing behaviors of TiO_2-supported Au overlayers, but also provides an effective strategy for the development of innovative sensor devices for H_2S recognition in the environment.

Keywords: *Density functional theory; H_2S; TiO_2-supported Au nanoparticle; PDOS*
© 2017 Published by Journal of Nanoanalysis.

INTRODUCTION

Over the past decades, TiO_2 (titania) has been demonstrated to be one of the most important transition metal semiconductors, which has various positive properties such as non-toxicity, high catalytic efficiency and wide band-gap [1]. It is a well-known metal oxide field effect transistor with a wide variety of applications in many fields such as photo-catalysis, gas sensor devices, organic dye-sensitized solar cells, water-splitting and environmental protection [2-5]. TiO_2 has three important polymorphs, namely anatase, rutile, and brookite [6].

Among these three polymorphs of TiO_2, the rutile polymorph is the most stable phase. There exists no exhaustive theoretical study on the physical and chemical properties of brookite due

* Corresponding Author Email: *a_abbasi@azaruniv.edu*

to its metastable nature, which leads to some difficulties during the synthesis of brookite [7]. It has been suggested that the anatase phase has more reactivity than the rutile and brookite phases in many catalytic reactions [8-14]. Anatase has been widely investigated owing to its improved activity in some photocatalysis reactions such as TiO$_2$ supported metal particle reactions, compared to the rutile and brookite phases [15-17]. The wide band gap (3-3.2 eV) of TiO$_2$ is the major concern associated with TiO$_2$, which not only affects its application in gas sensor devices, but also limits the response to the incoming solar light (absorption of 3-5 % of the spectrum). Nowadays, an eminent surge of interest has arisen in researching for methods to improve the photocatalytic activity of TiO$_2$. One of the most important strategies is nonmetal (nitrogen) doping, which extends the optical sensitivity of TiO$_2$ to the visible area [8].

Gold (Au) was traditionally considered as an improbable candidate for oxidation catalysts due to its inability to adsorb and dissociate oxygen. This opinion has changed significantly since gold nanoparticles supported on metal oxides such as TiO$_2$ were discovered. The nanoparticles supported on oxides exhibit excellent catalytic activity for low temperature CO oxidation [18, 19], and other useful reactions [20]. Numerous experimental and theoretical studies have been conducted to discover the basis of catalytic activity of gold catalysts [20], especially the position of active sites on the gold clusters. It is mostly observed that the oxidation of CO molecule takes place along the perimeter of the Au/oxide interface ('perimeter hypothesis') [21].

The gold particles supported on metal oxides (Oxide-supported gold particles) have fascinated huge attention owing to their greater activities in the surface processes [22-27]. Oxide-supported Au nanoparticles can be applied in several important applications such as epoxidation of propane [28], reduction of nitrogen oxides [29] and dissociation of sulfur dioxide molecule [30]. TiO$_2$ has been considered as one of the most appropriate support materials for gold particles [31, 32]. The interactions of gold nanoparticles with TiO$_2$ (rutile and anatase) have been widely studied in the last few years. Vittadini et al. Studied the adsorption of gold clusters on the TiO$_2$ anatase (101) surfaces [33]. Metiu and co-workers examined the adsorption site and

electronic structures of TiO$_2$ rutile supported Au nanoparticles [34]. The removal of harmful materials by adsorption and interaction over appropriate substrates has attracted great attention [35, 36]. In this regard, TiO$_2$ and based nanostructures have been used as efficient candidates for the removal of toxic gas molecules [37-41]. Recognition of harmful gas molecules is enormously vital and critical to public health and environmental security. Hydrogen sulfide is a toxic molecule and should be either removed or reduced to an environmentally acceptable value in the atmosphere. In this regard, TiO$_2$ supported Au nanoparticles have been well modified and are capable of detecting harmful H$_2$S molecules in the environment [42, 43].

A perfect semiconductor oxide based gas sensor should possess properties such as high sensitivity to the expected toxic material, low price fabrication and compatibility with modern electronic devices. Among the studied gas sensor materials, oxide supported gold nanoparticles have been considered as effectual sensor materials by the virtue of their greater activities. The mechanism of gas sensing for the removal of toxic H$_2$S molecules by metal oxide based sensors was represented in Figure 1.

In this study, therefore, H$_2$S interaction with TiO$_2$ supported Au nanoparticles were investigated by DFT calculations in order to determine the adsorption behaviors of these multicomponent heterostructure materials. The objective is to perform a systematic investigation on the adsorption behaviors of TiO$_2$-supported Au nanoparticles as potentially efficient gas sensors for H$_2$S detection.

COMPUTATIONAL METHODS
Details of Computation

Total energies and optimized geometries were explained using density functional theory calculations [44, 45] as implemented in the Open source Package for Material explorer (OPENMX3.8) [46]. OPENMX is an efficient software package for nano-scale materials, simulations based on norm-conserving pseudopotantials and pseudo-atomic localized basis functions [47, 48]. The pseudo atomic orbitals (PAOs) centered on the atomic sites were used as basis sets. For PAO functions, the database version 2013 was used. The energy cutoff of 150 Ry was set during the calculations. Pseudo-atomic orbitals were constructed by

minimal basis sets (3-s, 3-p and 1-d for the Ti atom), (3-s, 3-p, 2-d and 1-f for the Au atom), (3-s, 3-p for the S atom) and (2-s, 2-p for the O and N atoms), within cutoff radii of basis functions set to the values of 7 for Ti, 9 for Au, 8 for S, 5 for O and N (all in Bohrs). The exchange-correlation functional parameterized by Perdew, Burke, and Ernzerhof was employed [49]. Mulliken population analysis was also conducted in order to fully analyze the charge transfer between the H_2S and TiO_2 supported Au nanoparticle. The size of the simulation box containing pristine TiO_2-supported Au nanoparticles are 20 Å×20 Å×30 Å, which is much larger than the real size of the adsorption system. We have investigated four possible locations of the H_2S molecule near to the TiO_2-supported Au nanoparticles.

XCrysDen program was used for visualization of the figures presented in this study [50]. The considered TiO_2 supported Au nanoparticle contains 88 atoms (16 Au, 48 O and 24 Ti atoms)

of undoped TiO_2 supported Au overlayer. It is well known that the inclusion of dispersion correction is of high importance during the study of adsorption properties of different molecules on various surfaces, which correctly determines the adsorption energies and possible geometries of adsorbates over the surfaces. For this purpose, Grimme's DFT-D2 [51] method was employed in this study in order to take into account the effect of long range van der Waals interaction. The adsorption energy, E_{ad}, is estimated as the following equation:

$$E_{ad} = E_{(particle+adsorbate)} - E_{particle} - E_{adsorbate} \tag{1}$$

Where, $E_{(particle+adsorbate)}$ and $E_{particle}$ are the total energies of TiO_2-supported Au overlayers with and without adsorbed H_2S molecule, respectively. $E_{adsorbate}$ represents the energy of a free gas phase H_2S molecule. According to this definition, the adsorption energies of stable configurations would be negative.
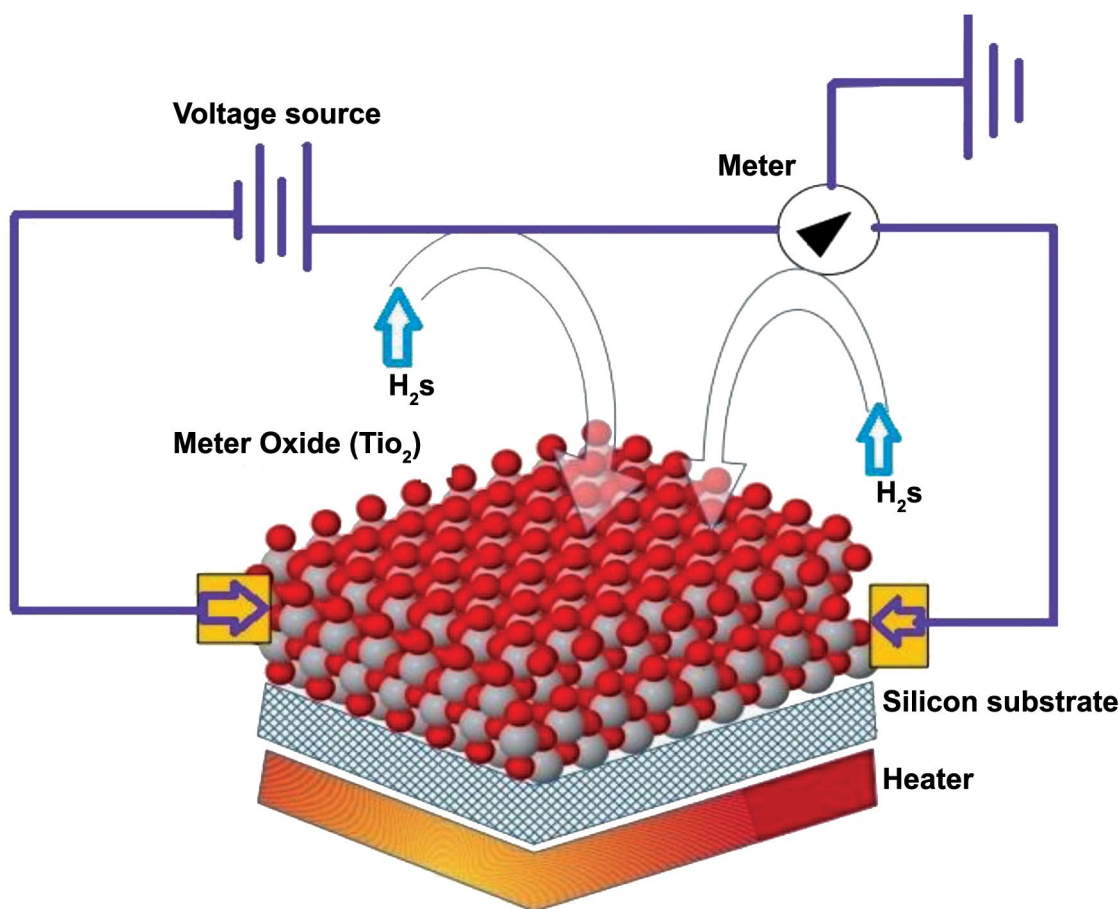

Fig. 1. Schematic representation of a typical TiO_2 based sensor device for H_2S detection in the environment.

Modeling TiO₂-supported Au nanoparticles

We have constructed TiO₂ anatase nanoparticle by using a 3×2×1 supercell of TiO₂ anatase. The considered unit cell is available at "American Mineralogists Database" webpage [52] and, reported by Wyckoff [53]. The size of the studied nanoparticles was chosen following Lei et al. [54] and Liu et al. [55]. They have explained that the nanoparticles containing 72 atoms have the lowest energy (highest stability) among the different type of nanoparticles. The optimized structure of the pristine TiO₂ nanoparticle was displayed in Figure 2.

bohr. TiO₂ possesses two types of titanium atoms, namely five-fold coordinated (5f-Ti) and six-fold coordinated (6f-Ti), as well as two types of oxygen atoms, indicated by three-fold coordinated (3f-O) and two-fold coordinated (2f-O) atoms [56,57].

Gas-phase H₂S molecule has a bent geometrical structure with S-H bond length of 1.34 Å and H-S-H bond angle of 92.1°, calculated from GGA method. These results are very close to the theoretically reported data [42]. The optimized structure of gas phase H2S molecule was shown in Figure 3. Figure 4 also displays the equilibrium structure of the undoped TiO₂-supported Au nanoparticle.

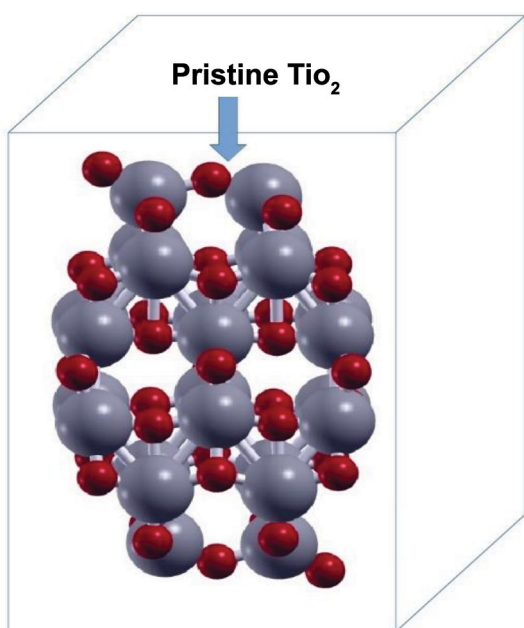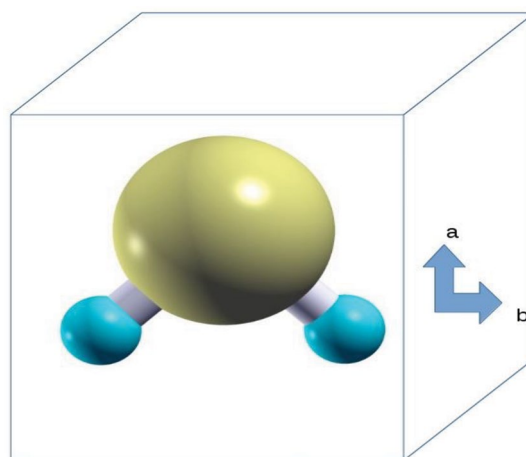

Fig. 2. Representation of a pristine TiO₂ anatase nanoparticle, two dangling oxygen atoms were used in order to set a 1:2 atomic number ratio between the oxygen and titanium atoms.

Fig. 3. Optimized structure of a gas phase H₂S molecule in a large cubic supercell.

The constructed structure of pristine TiO₂ nanoparticle was geometrically optimized and then coupled with Au nanoparticle in order to model a metal oxide supported Au overlayer. The atomic number ratio between titanium and oxygen atoms is set at 1:2, which was obtained by setting two dangling oxygen atoms in the TiO₂. Spin polarization is not used for the optimization of pristine TiO₂ particles. During the optimization process, "Cluster" method was used as efficient eigenvalue solver. For electronic structure calculations, the convergence criterion of 1.0×10^{-6} Hartree was used, whereas the criterion for geometry optimization was set at 1.0×10^{-4} Hartree/
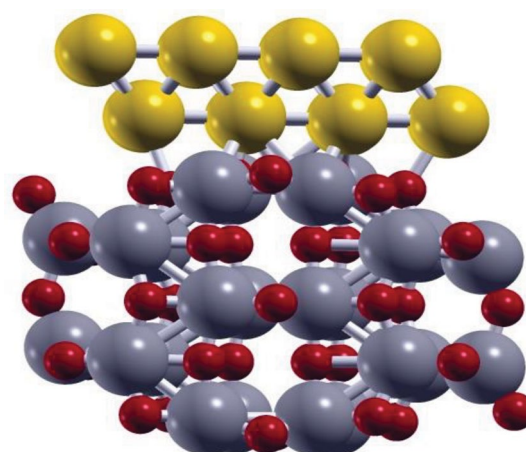

Fig. 4. The Optimized structure of pristine TiO₂ supported Au overlayer. The yellow, gray and red balls denote gold, titanium and oxygen atoms, respectively. TiO₂ was confirmed to be a suitable support material for Au.

RESULT AND DISCUSSION

Structural Parameters and Adsorption Energies

We begin by confirming that H$_2$S molecule can be adsorbed on both the Au and fivefold coordinated titanium sites of TiO$_2$ supported Au overlayers. Figures 5 and 6 show the equilibrium positions for H$_2$S placed above the Au and titanium sites of nanoparticle.

The sulfur atom of H$_2$S molecule binds preferentially to the fivefold coordinated titanium atom of TiO$_2$. There is not any mutual interaction between the hydrogen atoms of H$_2$S molecule and nanoparticle. The results suggest that the binding of H$_2$S to the fivefold coordinated titanium site is more energetically favorable than the binding to the Au site. Thus, the interaction of H$_2$S with TiO$_2$ side of nanoparticle is stronger than the interaction with Au side. This higher interaction gives rise to higher binding between the nanoparticle and adsorbate. The undercoordinated titanium sites are strongly

favored during the adsorption process. Different configurations of H$_2$S over the TiO$_2$ supported Au nanoparticles were obtained by placing H$_2$S molecule in different orientations towards the nanoparticle.

Configuration A shows the adsorption of H$_2$S on the top-Au site of the TiO$_2$ supported Au, whereas configurations B-D represent the interaction of H$_2$S with the fivefold coordinated titanium site of TiO$_2$. In configuration B, the H$_2$S molecule interacts with the O$_C$-substituted nanoparticle, while configuration C shows the reaction of H$_2$S with O$_T$-substituted one. H$_2$S molecule can also bind to the pristine nanoparticle, as displayed in configuration D. All of these configurations provide a single contacting point between the H$_2$S molecule and TiO$_2$ supported Au overlayer. Table 1 summarizes the lengths and distances for the newly formed Au-S and Ti-S bonds, S-H bonds of the adsorbed H$_2$S molecule and H-S-H bond angles of H$_2$S after the adsorption process.
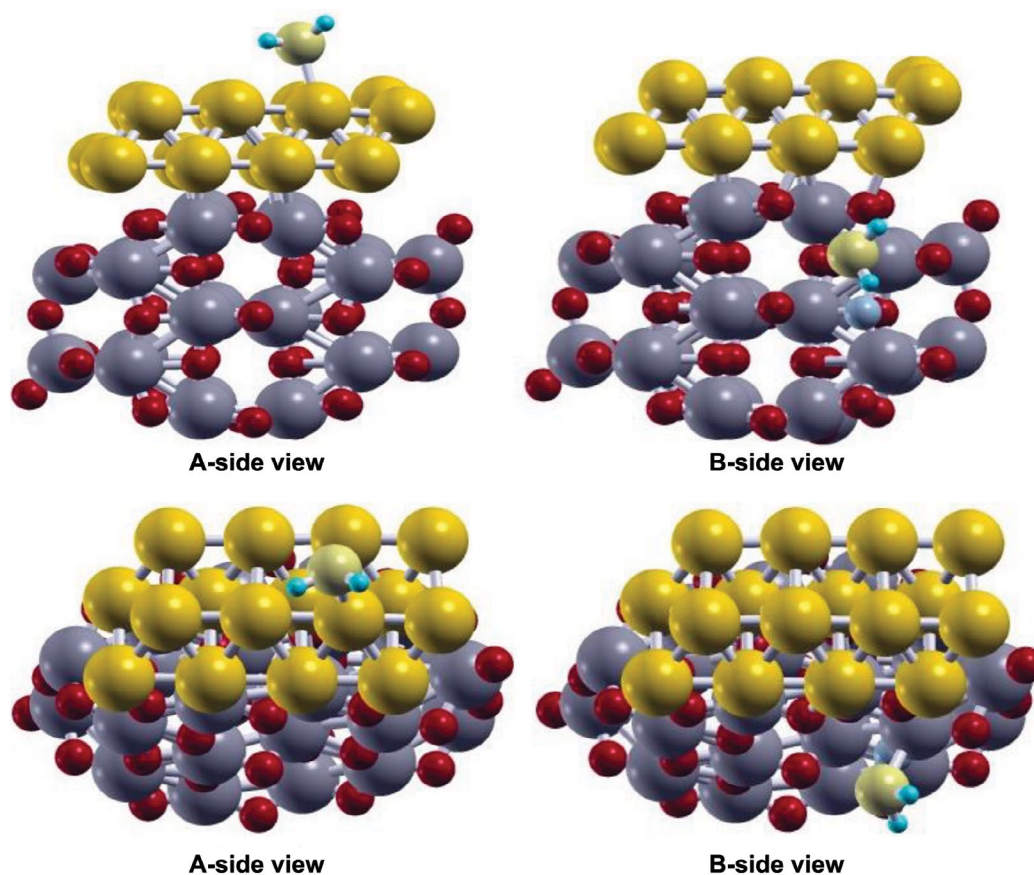

Fig. 5. Optimized geometry configurations of the H$_2$S adsorbed undoped and N-doped TiO$_2$ supported Au overlayers, (A) H$_2$S adsorption on the top Au site, (B) H$_2$S adsorption on the side Ti site of nitrogen substituted nanoparticle.
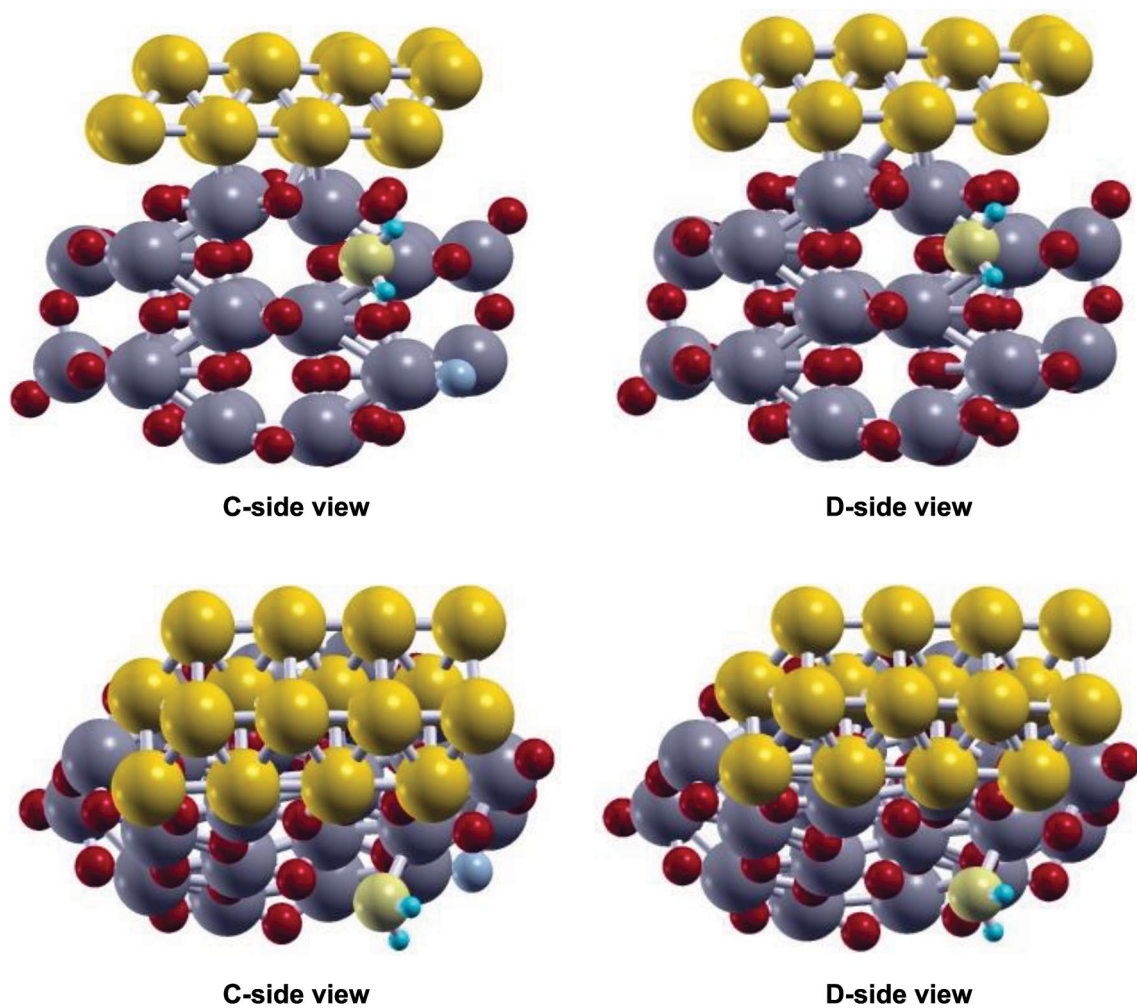
C-side view **D-side view**

C-side view **D-side view**

Fig. 6. Optimized geometry configurations of the H$_2$S adsorbed undoped and N-doped TiO$_2$ supported Au overlayers, (C) H$_2$S adsorption on the side Au site of nitrogen substituted nanoparticle, (B) H$_2$S adsorption on the side Au site of pristine nanoparticle.

Table 1. Bond lengths (in Å) and angles (in degrees) of H$_2$S molecule adsorbed on the TiO$_2$ supported Au nanoparticles

Complex type	Ti-S	S-H1	S-H2	H-S-H	Au-S
Undoped					
A	---	1.40	1.41	95.0	2.72
B	2.71	1.40	1.40	95.6	---
C	2.73	1.40	1.40	95.5	---
D	2.77	1.40	1.41	95.3	---
Non-adsorbed	---	1.34	1.34	92.1	---

The bond length variations indicate that the S-H bonds of the adsorbed H$_2$S molecule were elongated after the adsorption process, which can be ascribed to the considerable electronic density transfer from the Au-Au bonds of Au nanoparticle and S-H bonds of the H$_2$S molecule to the newly-formed bonds between the nanoparticle and H$_2$S. Thus, the adsorption process leads to weakening the S-H bonds of the H$_2$S molecule. The H-S-H bond angles of the H$_2$S molecule were increased compared to a free H$_2$S molecule in the gas phase. This increase in the bond angles could be mostly attributed to the elongation of the S-H bonds of the adsorbed H$_2$S molecule. This bond angle increase and obtained geometry variations could be ascribed to the formation of new bonds at the interface region. This formation of new bond is responsible for changing the sp hybridization of the sulfur atom in the H$_2$S molecule to hybridization with higher p contribution (near-sp^2). Consequently the p characteristics of bonding molecular orbitals of the sulfur atom in the adsorbed H$_2$S molecule increases.

Table 2 lists the adsorption energies of H$_2$S molecules on the pristine and N-doped TiO$_2$ supported Au nanoparticles. A clear comparison of the results indicates that the interaction of H$_2$S with N-doped nanoparticle is more energetically favorable than the interaction with undoped one. Therefore, the N-doped TiO$_2$ supported Au nanoparticle can react with H$_2$S molecule more strongly. Of the four configurations, configuration B has the highest value of adsorption energy, thus making it the most favorable binding of H$_2$S to the nanoparticle and consequently the most likely adsorption site to be occurred on the TiO$_2$ supported Au.

Table 2. Adsorption energies (in eV) and Mulliken charge values (in e) for H$_2$S molecule adsorbed on TiO$_2$ supported Au overlayers

Configuration	ΔE_{ad}		ΔQ
	PBE	DFT-D2	
Undoped			
A	-1.68	-2.22	-0.222
B	-2.12	-3.48	-0.224
C	-2.06	-3.36	-0.216
D	-1.80	-2.28	-0.202

The lowest adsorption energy belongs to configuration A, which represents the adsorption of H$_2$S on the Au site of pristine nanoparticle. Besides, the adsorption energy of configuration B is higher than that of configuration C, indicating that O$_C$-substituted nanoparticle can react with H$_2$S molecule more efficiently. Upon doping nitrogen atom into the threefold coordinated oxygen site (central oxygen site), the adsorption energy was improved with respect to the pristine nanoparticle.

By considering these results, we found that the nitrogen doping is an efficient strategy in order to strengthen the adsorption of H$_2$S on the TiO$_2$ supported Au nanoparticle. In other words, substituting of nitrogen atom into oxygen vacancy of TiO$_2$ is conductive to the interaction of H$_2$S with the considered nanoparticle. The adsorption energies are significantly increased when the effects of vdW interactions were taken into account. Tamijani et al .[53] reported the results of the adsorption of noble-gas atoms on the TiO$_2$ (110) surface based van der Waals corrected DFT approach and clearly demonstrated the increase in the adsorption energies caused by vdW interactions. The higher adsorption energy gives rise to a strong interaction between the adsorbent and adsorbed molecule, and its more negative sign also represents an energy favorable process. Thus, H$_2$S interaction with nitrogen modified TiO$_2$ supported Au nanoparticle is more favorable in energy than the interaction with intrinsic nanoparticle. Hence, the N-doped nanoparticle can be effectively utilized for the detection of toxic H$_2$S molecules in the environment.

Electronic Structures

Figure 7 displays the projected density of states (PDOSs) for H$_2$S adsorbed on the pristine and N-doped TiO$_2$ supported Au overlayers.

Panel (a) in this figure shows the PDOSs of the Au atom of gold nanoparticle and sulfur atom of the H$_2$S molecule (configuration A), while panels (c-d) represent the PDOS plots of the titanium and sulfur atoms for configurations B-D. The large overlaps between the PDOSs of the sulfur and titanium atoms indicate that the fivefold coordinated titanium atom forms a chemical bond with the sulfur atom of the H$_2$S molecule. By considering these considerable overlaps between the PDOSs of the interacting atoms, we found that H$_2$S molecule was chemisorbed on the nanoparticle. In order to further analyze the electronic structure of the adsorption systems, we have presented the PDOSs of five d orbitals of the titanium atom and the sulfur atoms of the H$_2$S molecule. Figure 8 shows the PDOSs of the sulfur atom of the H$_2$S molecule and different d orbitals of the titanium atom, representing significant overlaps between the PDOSs of the sulfur atom and d^1 orbital of the titanium atom.
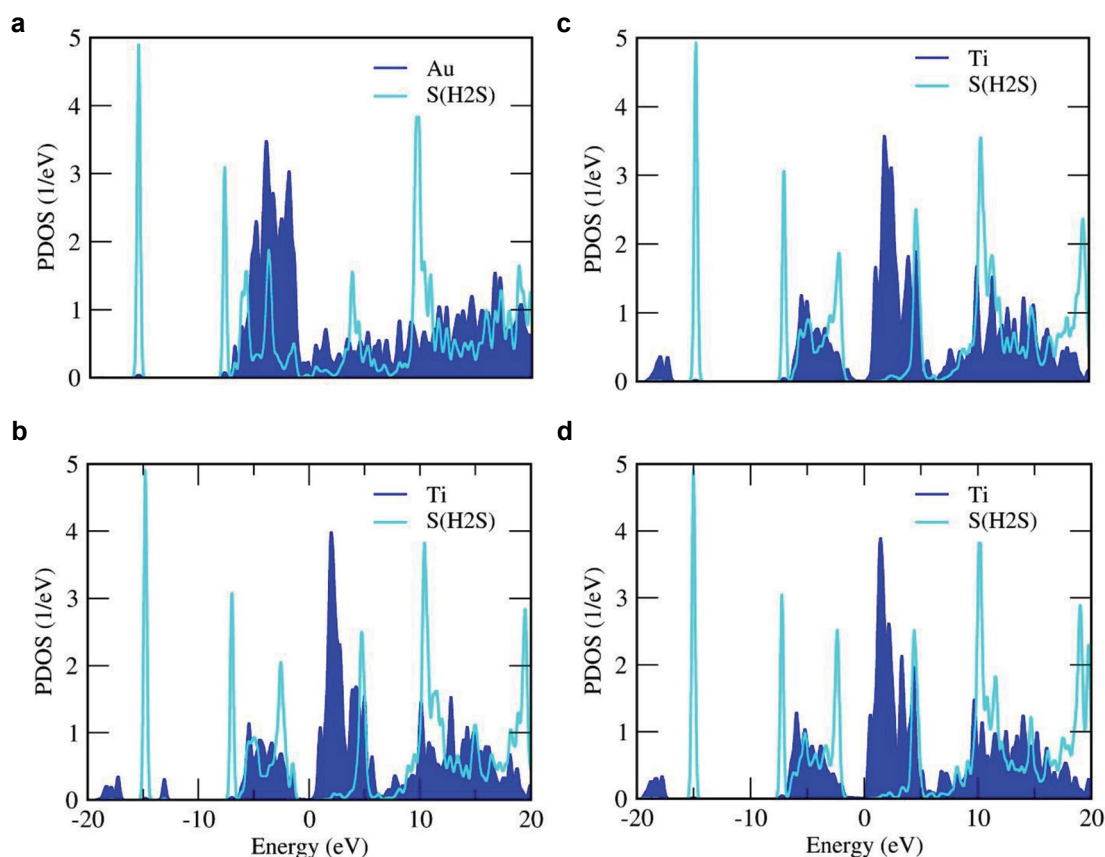
Fig. 7. PDOSs for the adsorption complexes of undoped TiO$_2$ supported Au nanoparticles with adsorbed NO$_2$ molecules. (a) Configuration A; (b) Configuration B; (c) Configuration C; (d) Configuration D.

This indicates that the sulfur atom has a large mutual interaction with the d^1 orbital of the titanium atom. Also, Figure 9 displays the PDOSs of the titanium atom of the nanoparticle and different orbitals of the sulfur atom.

This figure represents noticeable overlaps between the PDOSs of titanium atom and p^1 orbital of the sulfur atom.

Mulliken Charge Analysis

The charge transfer analysis between the adsorbate and adsorbent is a key issue that should be explained in detail during the adsorption of various gas molecules on the surfaces of materials. One of the most efficient methods is the Mulliken population analysis, which describes the charge exchange between the nanoparticle and adsorbed molecule. This method of charge analysis provides a means of estimating partial atomic charges from calculations implemented by computational chemistry packages. The calculated charge transfers were listed in Table 2. This method assigns an electronic charge to a given atom in the

considered system, that is, the gross atom population (GAP). The charge difference, ΔQ_A, is a measure of the difference between the number of electrons in the isolated free atom (Z_A), and the gross atom population:

$$\Delta Q_A = Z_A - GAP_A \qquad (2)$$

As a matter of convenience, we only discuss the charge transfer for complex B. For configuration B, the calculated charge transfer is about -0.224 |e| (e, the electron charge). The charge was transferred from the H$_2$S molecule to the TiO$_2$ supported Au nanoparticle, implying that H$_2$S behaves as a charge donor. Important to note is that the charge exchange between adsorbent and adsorbed molecule gives rise to variations on the conductivity of the system, being a helpful feature in order to develop more appropriate sensor devices for H$_2$S detection in the air. As can be seen from Table 2, the highest charge transfer occurs in configuration B, while the lowest charge transfer belongs to configuration D, in reasonable agreement with the trend of adsorption energy variations.
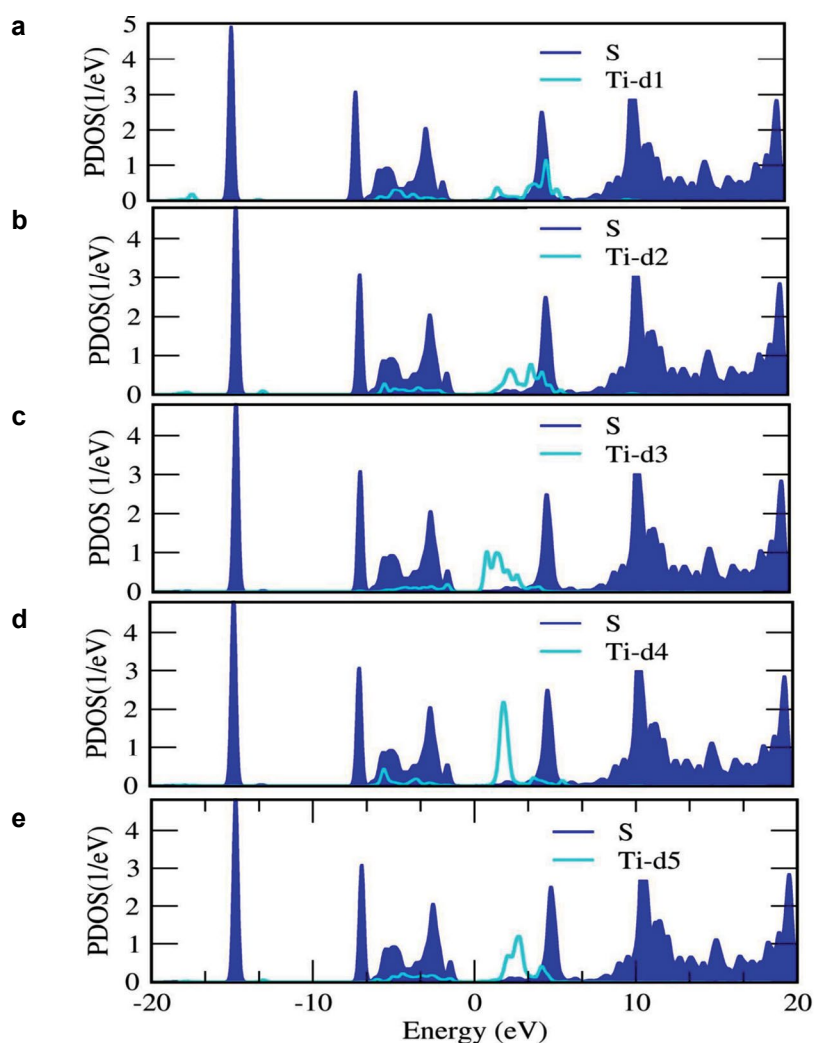
Fig. 8. PDOSs of the sulfur atom of H$_2$S molecule and five d orbitals of the titanium atom for TiO$_2$ supported Au overlayers with adsorbed H$_2$S molecules (configuration B).

One of the most important concerns associated with Mulliken charge analysis is the strong sensivity of Mulliken charges to the basis set choice. Basically, a complete basis set for a molecule can be covered by placing a large set of functions on a single atom. In the Mulliken scheme, all the electrons would then be assigned to the single atom. In Mulliken charge approach, there exists no efficient convergence for charges, and different basis set families may produce different results. In order to solve this problem, various effective methods have been proposed such as electrostatic potential and natural population methods [59]. We have also calculated the Mulliken charge values for the interacting titanium and sulfur atoms. The obtained results were summarized in Table 3. As

can be seen from this table, the fivefold coordinated titanium atom was positively charged, whereas the sulfur atom of the H$_2$S molecule carries a negative charge on its surface.

Table 3. Calculated Mulliken charge values for interacting atoms of the adsorption configurations of H$_2$S on the TiO$_2$ supported au overlayers

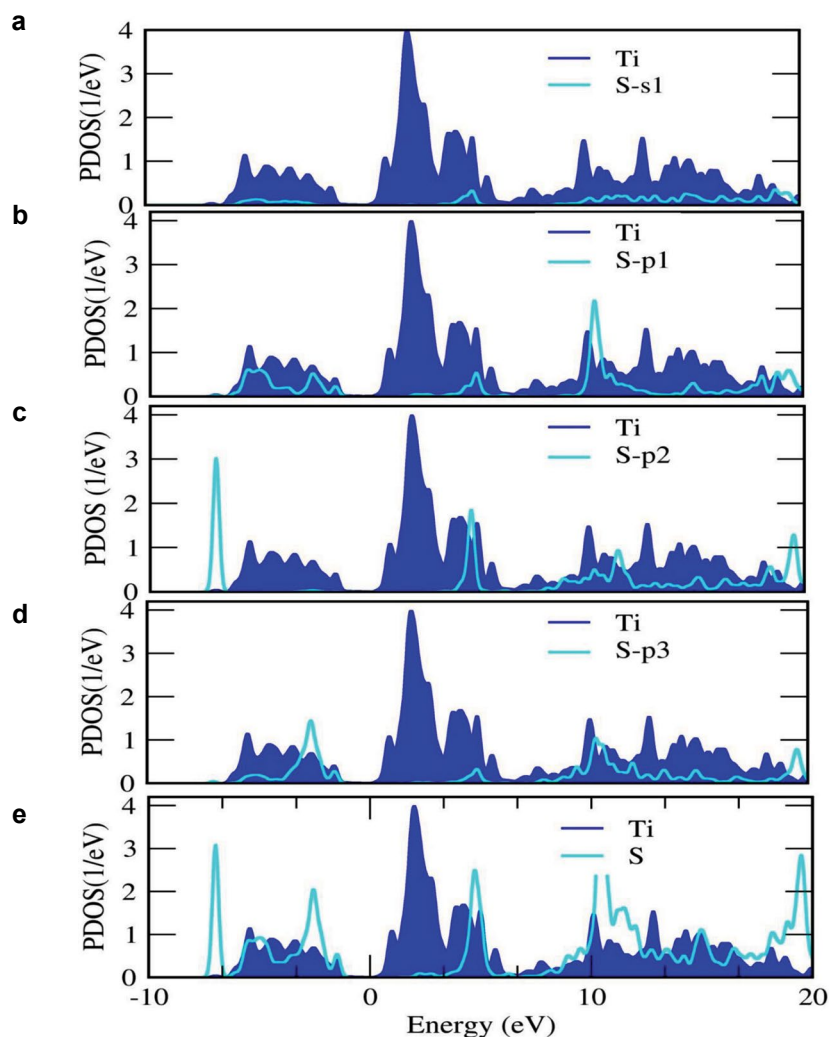| Configuration	Ti	S
B	+0.593	-0.258
C	+0.620	-0.266
D	+0.644	-0.273

Figure 9. PDOSs of the titanium atom, sulfur atom of H₂S molecule and different orbitals of the sulfur atom for TiO₂ supported Au overlayers with adsorbed H₂S molecules (configuration B).

CONCLUSION

We have performed DFT calculations for H₂S adsorption on the undoped and N-doped TiO₂ supported Au nanoparticles in order to fully exploit the gas sensing capability of these nanoparticles. H₂S molecule was located in different ways with respect to the nanoparticle. The results show that the S-H bonds of the adsorbed H₂S molecule were elongated after the adsorption process, which indicates the weakening S-H bonds of the H₂S molecule. The results also suggest that the interaction of H₂S molecule with N-doped TiO₂ supported Au overlayer is energetically more favorable than the interaction with undoped one. This interaction provides a single contacting point

between the H₂S and TiO₂ supported Au. Therefore, the N-doped TiO₂ supported Au nanoparticle can act as an ideal H₂S sensor in the environment. The substantial overlaps between the PDOSs of the titanium and sulfur, as well as, Au and sulfur atoms indicate the formation of chemical bonds between them. The charge analysis based on Mulliken charges reveals a noticeable charge transfer from the H₂S molecule to the TiO₂ supported Au nanoparticle, indicating the donor property of the H₂S molecule. By including vdW interaction, we found that the adsorption energies increase, which represents the dominant effect of long range vdW interaction. As a result, our findings thus suggest that the nitrogen modified TiO₂

supported Au nanoparticle would be a highly efficient H$_2$S sensor.

CONFLICT OF INTEREST

The authors declare that there is no conflict of interests regarding the publication of this manuscript.

REFERENCES

1. A. Fujishima and K. Honda, Nature. 238, 37 (1972).

2. A. Fujishima, K. Hashimoto, and T. Watanabe, TiO$_2$ Photocatalysis: Fundamentals and Applications, Bkc, Tokyo, (1999).

3. A. Abbasi and J.J. Sardroodi, Environ. Sci.: Nano. 3, 1153 (2016).

4. A. Abbasi and J.J. Sardroodi, Comp. Theor. Chem. 600, 2457 (2016).

5. A. Fujishima, X. Zhang and D.A. Tryk, Surf. Sci. Reports, 63, 515 (2008).

6. M. Batzilla, E.H. Morales, and U. Diebold, J. Chem. Phys. 339, 36 (2007).

7. S.L. Isley and R.L. Penn, J. Phys. Chem. B. 110, 15134 (2006).

8. A.K. Rumaiz, J.C. Woicik, E. Cockayne, H.Y. Lin, G.H. Jaffari, and S. I. Shah, J. Appl. Phys. Letts. 95, 262111 (2009).

9. R. Buonsanti, V. Grillo, E. Carlino, C. Giannini, T. Kipp, R. Cingolani and P.D. Cozzoli, J. Am. Chem. Soc. 130, 11223 (2008).

10. S. Cassaignon, M. Koelsch and J.P. Jolivet, J. Mater. Sci. 42, 6689 (2007).

11. A. Di Paola, M. Addamo, M. Bellardita, E. Cazzanelli and L. Palmisano, Thin Solid Films. 515 (7), 3527 (2007).

12. Y. Djaoued, R. Bruning, D. Bersani, P.P. Lottici and S. Badilescu, Mater. Lett. 58(21), 2618 (2004).

13. F. Iskandar, A.B.D. Nandiyanto, K. M.Yun, C.J. Hogan, K. Okuyama and P. Biswas, Adv. Mater. 19, 1408 (2007).

14. M. Kobayashi, V.V. Petrykin and M. Kakihana, Chem. Mater. 19, 5373 (2007).

15. J.G. Li, T. Ishigaki and X.D. Sun, J. Phys. Chem. C. 111, 4969 (2007).

16. M.A. Reddy, M.S. Kishore, V. Pralong, V. Caignaert and U.V. Varadaraju, Electrochemistry communications. 8(8), 1299 (2006).

17. Y. Shibata, H. Irie, M. Ohmori, A. Nakajima, T. Watanabe, and K. Hashimoto, Phys. Chem. Chem. Phys. 6, 1359 (2007).

18. M. Haruta, N. Yamada, T. Kobayashi and S. Iijima, J. Catal. 115, 301 (1989).

19. M. Okumura, S. Nakamura, S. Tsubota, T. Nakamura, M. Azuma and M. Haruta, Catal. Lett. 51, 53 (1998).

20. T. Takei, T. Akita, I. Nakamura, T. Fujitani, M. Okumura, K. Okazaki, J.H. Huang, T. Ishida and M. Haruta, Adv. Catal. 55, 1 (2012).

21. M. Haruta, Catal. Today 36, 153 (1997).

22. P. Landon, P.J. Collier, A.J. Papworth, C.J. Kiely, and G.J. Hutchings, Chem. Commun. 18, 2058 (2002).

23. L.M. Molina and B. Hammer, Appl. Catal. A Gen. 291, 21 (2005).

24. M. Okumura, S. Tsubota and M. Haruta, J. Mol. Catal. A Chem. 199, 73 (2003).

25. N. Lopez and J.K. Norskov, J. Am. Chem. Soc. 124, 11262 (2002).

26. M.S. Chen and D.W. Goodman, Catal. Today. 111, 22 (2006).

27. H.H. Kung, M.C. Kung and C.K. Costello, J. Catal. 216, 425 (2003).

28. T.M. Hayashi, K. Tanaka and M. Haruta, J. Catal. 178, 566 (1998).

29. T. Salama, R. Ohnishi, T. Shido and M. Ichikawa, J. Catal. 162(2), 169 (1996).

30. J.A. Rodriguez, G. Liu, T. Jirsak, J. Hrbek, Z.P. Chang, J. Dvorak and A. Maiti, J. Am. Chem. Soc. 124, 5242 (2002).

31. M.S. Chen and D.W. Goodman, Science. 306(5694), 252 (2004).

32. F. Cosandey and T.E. Madey, Surf. Rev. Lett. 8, 73 (2001).

33. A. Vittadini and A. Selloni, J. Chem. Phys. 117, 353 (2002).

34. S. Chrétien and H. Metiu, J. Chem. Phys. 127, 084704 (2007).

35. J. Azamat, A. Khataee and S. W. Joo, Journal of Molecular graphics and Modelling, 53, 112 (2014).

36. J. Azamat, A. Khataee and S. W. Joo, RSC Advances, 5(32), 25097 (2015).

37. A. Abbasi and J.J. Sardroodi, Int. J. Bio-Inorg. Hybr. Nanomater., 5, 43 (2016).

38. A. Abbasi and J. J. Sardroodi, Int. J. Nano Dimens., 7, 349, (2016).

39. A. Abbasi and J. J. Sardroodi, J. Water Environ. Nanotechnol., 2, 52 (2017).

40. A. Abbasi, J.J. Sardroodi and A. R. Ebrahimzadeh, J. Water Environ. Nanotechnol., 1, 55 (2016).

41. A. Abbasi and J.J. Sardroodi, Int. J. Bio-Inorg. Hybr. Nanomater., 5, 105 (2016).

42. S.F. Peng and J.J. Ho, J. Phys. Chem. C. 114, 19489 (2010).

43. N.M. Galea, E.S. Kadantsev, and T. Ziegler, J. Phys. Chem. C. 113,193 (2009).

44. P. Hohenberg and W. Kohn, Phys. Rev., 136, B864 (1964).

45. W. Kohn and L. Sham, Phys. Rev., 140, A1133 (1965).

46. The code, OPENMX, pseudoatomic basis functions, and pseudopotentials are available on a web site 'http://www.openmxsquare.org'.

47. T. Ozaki, J. Physical Review. B. 67, 155108 (2003).

48. T. Ozaki and H. Kino, Numerical atomic basis orbitals from H to Kr, Phys. Rev. B., 69, 195113 (2004)

49. J.P. Perdew and A. Zunger, Phys. Rev. B., 23, 5048 (1981).

50. A. Koklj, Comput. Mater. Sci., 28, 155 (2003).

51. S. Grimme, J. Comput. Chem., 27(15), 1787 (2006).

52. Web page at: http://rruff.geo.arizona.edu/AMS/amcsd.php.

53. R.W.G. Wyckoff. Crystal structures, Second edition. Interscience Publishers, USA, New York, (1963).

54. Y. Lei, H. Liu and W. Xiao, J. Modelling Simul. Mater. Sci. Eng., 18, 025004 (2010).

55. J. Liu, L. Dong, W. Guo, T. Liang and W. Lai, J. Phys. Chem. C. 117, 13037 (2013).

56. M. Lazzeri, A. Vittadini and A. Selloni, J. Phys. Rev. B. 63 155409 (2001).

57. C. Wu, M. Chen, A.A. Skelton, P.T. Cummings and T. Zheng, ACS Appl. Mat. Interfaces. 5, 2567 (2013).

58. A.A. Tamijani, A. Salam, and P. de-Lara-Castells, J. Phys. Chem. C. 120(32), 18126 (2016).

59. A.E. Reed, R.B. Weinstock and F. Weinhold, J. Chem. Phys. 83 (2), 735 (1985).